ISSN 1063-7826, Semiconductors, 2011, Vol. 45, No. 10, pp. 1281–1285. © Pleiades Publishing, Ltd., 2011.
Original Russian Text © V.V. Voitovych, V.B. Neimash, N.N. Krasko, A.G. Kolosiuk, V.Yu. Povarchuk, R.M. Rudenko, V.A. Makara, R.V. Petrunya, V.O. Juhimchuk, V.V. Strelchuk, 2011, published in Fizika i Tekhnika Poluprovodnikov, 2011, Vol. 45, No. 10, pp. 1331–1335.

SURFACES, INTERFACES, AND THIN FILMS

The Effect of Sn Impurity on the Optical and Structural Properties of Thin Silicon Films

V. V. Voitovych[a]^, V. B. Neimash[a], N. N. Krasko[a], A. G. Kolosiuk[a], V. Yu. Povarchuk[a], R. M. Rudenko[b], V. A. Makara[b], R. V. Petrunya[b], V. O. Juhimchuk[c], and V. V. Strelchuk[c]

[a] *Institute of Physics, National Academy of Sciences of Ukraine, Kyiv, 03650 Ukraine*

^ *e-mail: vvoitovych@yahoo.com*

[b] *Kyiv National University, Department of Physics, Kyiv, 03680 Ukraine*

[c] *Lashkaryov Institute of Semiconductor Physics, National Academy of Sciences of Ukraine, Kyiv, 03650 Ukraine*

Submitted January 31, 2011; accepted for publication March 16, 2011

Abstract—The effect of tin impurity on the structure and optical properties of thin-film amorphous silicon is investigated. It is established that tin impurity accelerates crystallization of amorphous silicon. Immediately after deposition of a film onto a substrate at a temperature of ~300°C, there is a crystalline phase of silicon in samples with tin. High-vacuum annealing at 350–750°C leads to growth of the crystalline phase in films with tin: nanocrystals grow in size from ~3.0 to 4.5 nm. At the same time, in films without tin, only the degree of the short-range order increases. Silicon film without tin remains amorphous over the entire range of annealing temperatures.

DOI: 10.1134/S1063782611100253

1. INTRODUCTION

In recent years increasing attention has been paid to studying the properties of thin silicon films with a two-phase structure, i.e., silicon nanocrystals in an amorphous silicon matrix. The parameters of such a material are more stable to light than those of amorphous silicon [1], which makes two-phase silicon films promising for application in optoelectronic devices, including solar cells. The physical properties of such films depend, to a great extent, on the ratio between the amorphous and crystal phases and size and the concentration of silicon nanocrystals in the amorphous matrix. Therefore, one important current technological problem is controlling the growth of one silicon phase in the other.

One of the known methods allowing the band gap of amorphous silicon to be affected is doping with isovalent impurities, such as Ge and C [2, 3]. The isovalent impurities of the IV Group do not create electrically active centers, but may radically affect the electrical parameters of Si upon thermal treatment and radiation [4–9]. In particular, heavy isovalent Sn and Pb impurities substantially affect the accumulation of radiation and thermal defects, which, in turn, determine radiation degradation and thermal instability of electrical conductivity and the carriers' lifetime in silicon [10–14]. In the available publications, there is a lack of experimental data on the effect of these impurities on the properties of thin-film Si in the amorphous and two-phase states.

This study was aimed at investigation of the effect of the isovalent tin impurity on the optical and structural properties of silicon films and the formation of the crystalline phase in amorphous thin-film silicon.

2. EXPERIMENTAL

Two sets of thin-film silicon samples were prepared by thermal evaporation of powders from a tantalum trough. Set I was obtained from KEF-4.5 single-crystal silicon; set II, from a mixture of KEF-4.5 single-crystal silicon (n-Si:P, $\rho = 4.5\ \Omega$ cm) and 99.92%-pure tin in the ratio 1 : 100. The films were grown in vacuum with a residual pressure of $\sim 10^{-5}$ Pa on silicon and quartz substrates. The substrate temperature during deposition was 300°C. The thickness of the silicon films measured with an MII-4 microinterferometer was ~750 nm.

The component composition of the silicon films was determined using an EXPERT 3L express analyzer based on energy-dispersive X-ray fluorescent analysis of substances.

To modify the structural and optical properties of the films of sets I and II, the samples were subjected to isochronous annealing in vacuum in the temperature range from 350 to 750°C with a step of 50°C. The annealing time at each temperature was 20 min.

Optical absorption spectra were measured for the initial and annealed films in the photon energy range $h\nu = 1.1$–1.9 eV. The absorption coefficient spectra of the films were calculated using the formula

$$\alpha = (1/d)\ln(I/I_0),$$

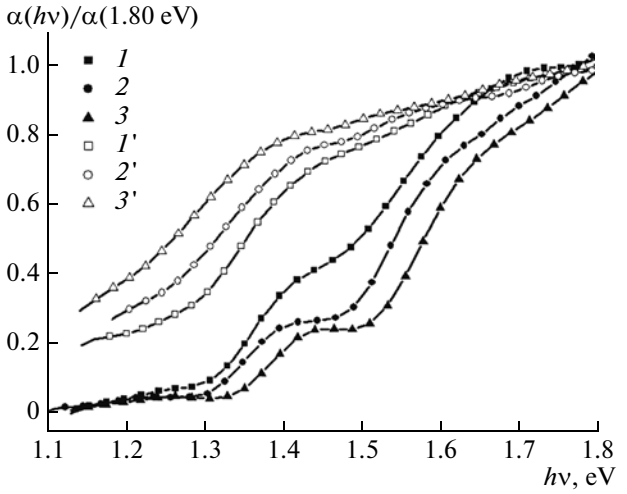

Fig. 1. Spectral dependences of the absorption coefficient in the relative units $\alpha(h\nu)/\alpha(1.80\ \text{eV})$ of the initial and annealed samples of thin-film silicon without tin (*1*–*3*) and with tin (*1'*–*3'*): initial samples (*1*, *1'*), samples annealed at 450°C (*2*, *2'*), and samples annealed at 700°C (*3*, *3'*).

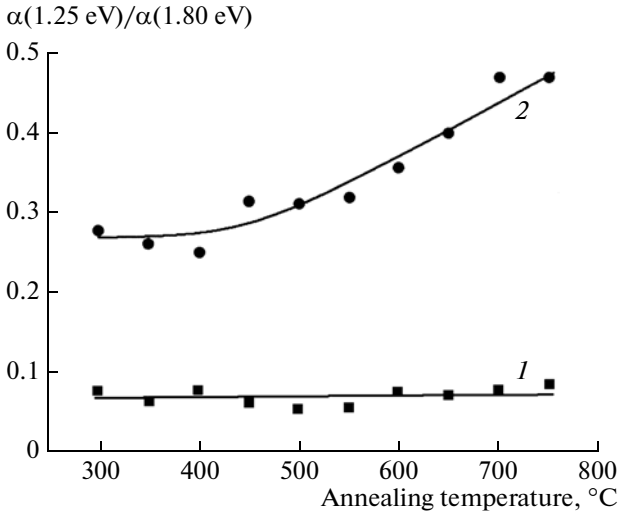

Fig. 2. Temperature dependences of the absorption coefficient at $h\nu = 1.25$ eV in the relative units $\alpha(1.25\ \text{eV})/\alpha(1.80\ \text{eV})$ for the samples of (*1*) *a*-Si and (*2*) *a*-Si:Sn/*nc*-Si.

where α is the absorption coefficient of a silicon film, *d* is the film thickness, *I* is the intensity of light passed through the silicon film and the quartz substrate, and I_0 is the intensity of light passed through the substrate. Using the spectral dependence of the optical absorption coefficient in the defect-related region of the spectrum, information on defect density in the films under study was obtained.

Raman spectra were recorded at room temperature using a T-64000 spectrometer (Jobin Yvon). The spectra were excited by an Ar^+ laser with a wavelength of 488 nm. All the measurements were performed at room temperature.

3. RESULTS AND DISCUSSION

The results of X-ray fluorescent analysis of the initial films showed that the samples from set II contain tin in a concentration that amounts to ~1% of concentration of Si atoms. Hereinafter, the thin-film silicon samples with tin are referred to as *a*-Si:Sn/*nc*-Si; the amorphous silicon samples, as *a*-Si.

Figure 1 shows the spectral dependences of the absorption coefficient in the relative units $\alpha(h\nu)/\alpha(1.8\ \text{eV})$ for the initial and annealed thin-film silicon samples without tin (curves *1*–*3*) and with tin (curves *1'*–*3'*). According to previous studies [15, 16], for the amorphous silicon films obtained under the same technological conditions, the absorption coefficients upon interband excitation (the photon energies are $h\nu \geq 1.8$ eV) are close to each other. The measurement of the relative absorption coefficient $\alpha(h\nu)/\alpha(1.8\ \text{eV})$ of the films under study reflects the variation in defect density in them.

It can be seen in Fig. 1 that, for the two different sets of the films, we observed markedly different absorption coefficients in the region of the so-called defect-related absorption ($h\nu < 1.5$ eV) determined by optical transitions in which the electron states of defects participate [15].

With an increase in the temperature of multistage high-vacuum annealing from 350 to 750°C, structural transformations and defect density variations occur in the films of both sets, which is reflected in the absorption spectra. In the initial *a*-Si:Sn/*nc*-Si films, the absorption at the interface between the amorphous and crystalline phases ($h\nu = 1.25$ eV) and absorption determined by the density of the electron states of defects ($h\nu = 1.4$ eV) appear larger compared to that observed in *a*-Si [15, 16]. With an increase in the annealing temperature, the optical absorption curve of the *a*-Si films shifts toward higher photon energies and the curve of *a*-Si:Sn/*nc*-Si shifts toward lower photon energies. Thus, the tin impurity in the amorphous silicon films affects the optical absorption spectrum considerably.

Temperature dependences of the absorption coefficient at $h\nu = 1.25$ eV for the samples under study are presented in Fig. 2 in relative units $\alpha(1.25\ \text{eV})/\alpha(1.8\ \text{eV})$. With increasing annealing temperature, the value of $\alpha(1.25\ \text{eV})/\alpha(1.8\ \text{eV})$ does not change for the *a*-Si samples and increases for *a*-Si:Sn/*nc*-Si.

The degree of crystallinity, average size of nanocrystals, and effect of heat treatment on the phase composition for films of both sets were studied by Raman spectroscopy.

Figures 3 and 4 present Raman spectra for the initial and annealed samples from set I. It can be seen that all the spectra of the annealed samples contain

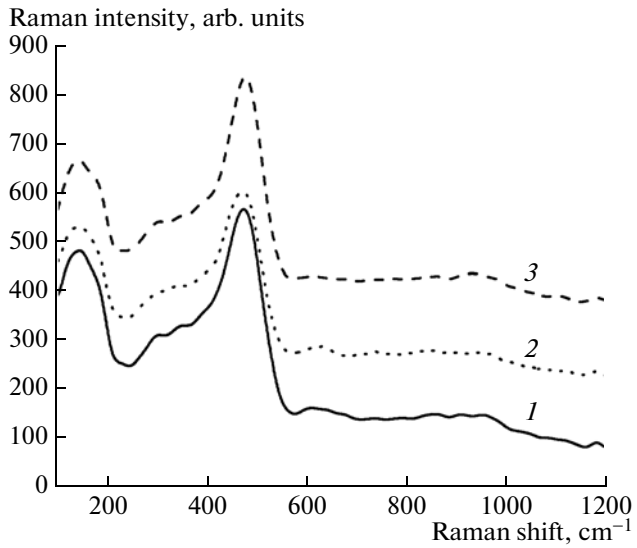

Fig. 3. Raman spectra of the *a*-Si samples (set I): (*1*) initial sample and samples annealed in vacuum at (*2*) 450 and (*3*) 700°C.

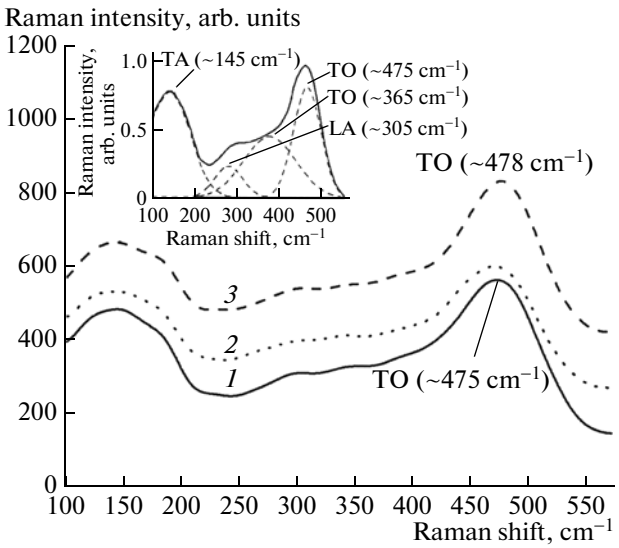

Fig. 4. Main bands of the Raman spectra of the *a*-Si samples (set I). Designation is the same as in Fig. 3. The insert shows decomposition of the bands of spectrum *1* into Gaussian components.

bands characteristic of amorphous silicon [17]: TA (~145 cm^{-1}), LA (~305 cm^{-1}), LO(~365 cm^{-1}), and TO(~475 cm^{-1}).

Variation in the frequency position and integrated intensity of the bands upon thermal annealing was analyzed after decomposition of the experimental spectra to the components (the insert in Fig. 4). The results obtained showed that, with increasing annealing temperature, the TO band slightly shifts to higher frequencies and its width at half-maximum decreases. It is assumed that the TO band width is determined by the dispersion of the angles of bonds between atoms, i.e., fluctuations of the latter in the short-range order [18]. Therefore, a decrease in the TO band width implies an increase in the degree of short-range ordering of silicon atoms in *a*-Si.

It was shown by Cody et al. [19] that there is a correlation between the ratio of the TA and TO band intensities I_{TA}/I_{TO} and the band gap E_g: the latter grows with decreasing I_{TA}/I_{TO}. The optical band gap in amorphous semiconductors is determined as [11]

$$E_g = E - D(\langle u^2\rangle_T - \langle u^2\rangle_x),$$

where E is the optical band gap of *a*-Si without structural disordering at the temperature $T = 0$ K, D is the deformation potential, $\langle u^2\rangle_T$ is the averaging over the ensemble of atomic displacements caused by thermal motion, and $\langle u^2\rangle_x$ is a similar quantity related to structural disordering. In our case, the value of I_{TA}/I_{TO} decreases from 1.42 to 1.29 with increasing annealing temperature. Such a variation in I_{TA}/I_{TO} may imply that the value of E_g increases for the *a*-Si samples with increasing temperature.

Quite a different situation is observed for the *a*-Si:Sn/*nc*-Si films. Immediately after deposition of a film at a substrate temperature of 300°C, a band with the maximum at ~512 cm^{-1} with an extended low-frequency wing is observed, which is typical of Si nanocrystals [20] (Fig. 5). With an increase in the annealing temperature from 450 to 700°C, the high-frequency shift of this band from 512 to 514 cm^{-1} is observed (Fig. 6).

In all the Raman spectra of the samples from set II, a broad band caused by Si–Sn oscillations arises near

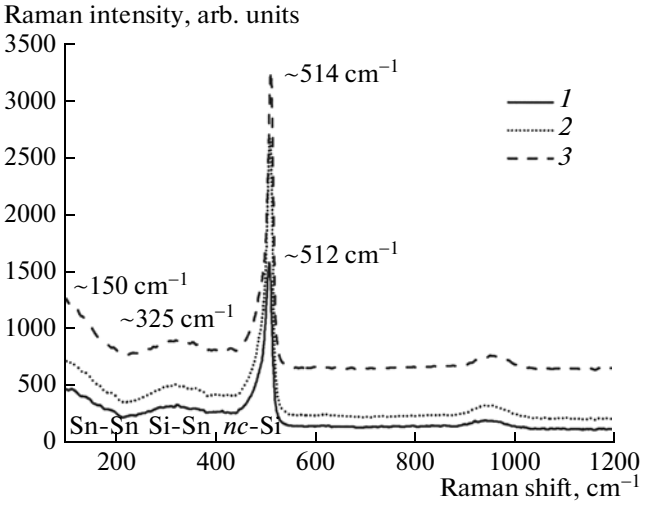

Fig. 5. Raman spectra of the *a*-Si:Sn/*nc*-Si samples (set II): (*1*) initial sample and samples annealed in vacuum at (*2*) 450 and (*3*) 700°C.

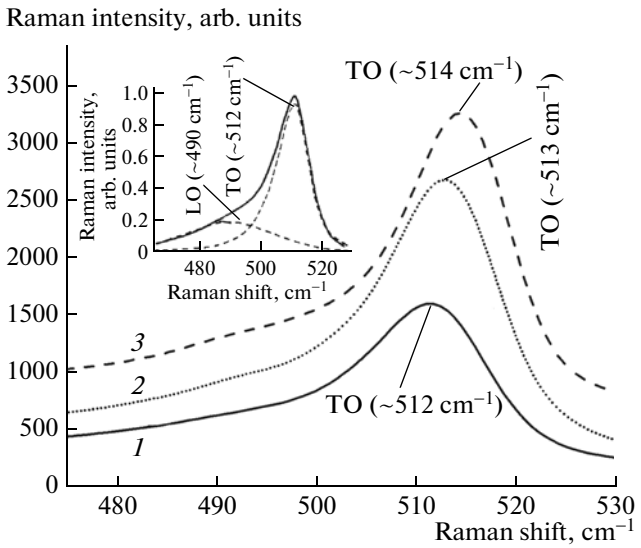

Fig. 6. Main band in Raman spectra of the *a*-Si:Sn/*nc*-Si samples (set II). Designation is the same as in Fig. 5. The insert shows decomposition of the band of spectrum *1* into Gaussian components.

325 cm^{-1} [21]. The position of this band is close to that of the LA band of amorphous silicon; however, the LA band has a lower frequency; in addition, in this case, the TO band should appear in the Raman spectra (the inset in Fig. 4). It must be noted that, in the region ~150 cm^{-1}, Sn–Sn oscillations contribute to the Raman spectrum [21]. Analysis of the experimental spectra shows that some of the Sn atoms can become incorporated into the silicon matrix, which causes the occurrence of the band corresponding to the Si–Sn oscillations or the Si–Sn bonds formed at the interface between tin nanoclusters and the silicon matrix. The intensity and frequency position of this band are nearly invariable with increasing annealing temperature. This means that the number of Si–Sn bonds does not increase with annealing temperature. As is known, Sn atoms are poorly soluble in silicon [22]; therefore, one may assume that they combine in individual nanoclusters, as a form more favorable energetically, already during the formation of the film.

To estimate the average size of silicon nanocrystals, we theoretically simulated the experimental bands corresponding to the Si–Si oscillations (insert in Fig. 6) by decomposition of the band with the maximum at ~512 cm^{-1} into two components describing the contributions of the oscillations of silicon nanocrystals LO (~490 cm^{-1}) and TO (~512 cm^{-1}).

The presence of both LO and TO oscillations of silicon nanocrystals in the Raman spectrum is caused by the fact that Si nanoclusters in the film volume have different orientation; therefore, both modes contribute to scattering. The individual bands were described by the formula [23, 24]

$$I(\nu) = \int \exp\left(-\frac{q^2 D^2}{16\pi^2}\right) \frac{d^3 q}{[\nu - \nu(q)]^2 + (\Gamma_0/2)^2},$$

where Γ_0 is the phonon band width of single-crystal Si and $\nu(q)$ are the dispersion dependences for the TO and LO oscillations. The average sizes of silicon nanocrystals estimated within the model from [24] are ~3.0 nm just after film deposition and ~4.5 nm after annealing at 700°C. Usually, one should take into account that there is a silicon-nanocrystal size spread in the film under investigation. In addition the film may contain an insignificant amount of amorphous silicon, which causes an error in the description of the experimental curve and, consequently, in determination of the average sizes of nanocrystals.

The results obtained show that doping of thin-film amorphous silicon with isovalent tin impurity considerably accelerates crystallization of the film. Even during film deposition at a substrate temperature of 300°C, the majority of the amorphous phase is transformed into the crystalline one, which is a substantial difference between these films and films without tin, the structure of which remains amorphous over the entire range of the annealing temperatures up to 700°C. An increase in absorption at $h\nu = 1.2$ eV in *a*-Si:Sn/*nc*-Si with the annealing temperature may originate from the formation and further growth of nanocrystalline silicon in such structures, which is in good agreement with the Raman scattering results.

The change in the value of I_{TA}/I_{TO} for *a*-Si, in contrast to *a*-Si:Sn/*nc*-Si is not related to phase transformation of the material. In this case an increase in I_{TA}/I_{TO} is caused by short-range ordering of Si atoms during heat treatment.

4. CONCLUSIONS

Based on the results of this study, we may conclude that doping of thin-film amorphous silicon with isovalent tin impurity leads to a considerable decrease in the temperature of crystallization of *a*-Si.

It was established that Sn–Sn and Si–Sn bonds are formed just after film deposition onto a substrate at a temperature of 300°C.

It was shown that isochronous high-vacuum annealing of the *a*-Si:Sn/*nc*-Si samples in the temperature range 300–700°C leads to an increase in the sizes of silicon nanocrystals from 3 to 4.5 nm.

It was experimentally established that the *a*-Si films undoped with tin remain amorphous over the entire annealing temperature range and a decrease in I_{TA}/I_{TO} may be caused by structural ordering during heat treatment.

REFERENCES

1. A. Shan, E. Vallat-Shauvain, P. Torres, J. Meier, U. Kroll, C. Hof, C. Droz, M. Goerlitzer, N. Wyrsch, and M. Vanechek, Mater. Sci. Eng. **69–70**, 219 (2000).
2. A. V. Vasin, A. V. Rusavskii, V. S. Lysenko, A. N. Nazarov, V. I. Kushnirenko, S. P. Starik, and V. G. Stepanov, Semiconductors **39**, 572 (2005).
3. A. V. Ershov, A. I. Mashin, A. F. Khokhlov, D. E. Kas'yanov, A. V. Nezhdanov, N. I. Mashin, and I. A. Karabanova, in *Proceedings of the 1st Workshop on NATO SfP-973799 Project Semiconductors* (Nizh. Novgorod, 2001), p. 124.
4. V. E. Kustov, M. G. Mil'vidskii, Yu. G. Semenov, B. M. Turovskii, V. I. Shakhovtsov, and V. L. Shindich, Sov. Phys. Semicond. **20**, 169 (1986).
5. V. M. Babich, N. I. Bletskan, and E. F. Venger, *Oxygen in Silicon Monocrystals* (Interpres LTD, Kiev, 1997), p. 240 [in Russian].
6. K. L. Brower, Phys. Rev. B **9**, 2607 (1974).
7. A. Mesli and A. Nylandsted Larsen, Phys. Rev. Lett. **83**, 148 (1999).
8. C. V. Budtz-Jorgensen, P. Kringhoj, A. Nylandsted Larsen, and N. V. Abrosimov, Phys. Rev. B **58**, 1110 (1998).
9. G. D. Watkins, Phys. Rev. B **12**, 4383 (1975).
10. V. B. Neimash, A. Kraitchinskii, M. Kras'ko, O. Puzenko, C. Claeys, E. Simoen, B. Svensson, and A. Kuznetsov, J. Electrochem. Soc. **147**, 2727 (2000).
11. V. B. Neimash, A. M. Kraitchinskii, M. M. Krasko, O. O. Pusenko, E. Simoen, C. Claeys, A. Blondeel, and P. Clauws, Ukr. J. Phys. **45**, 1121 (2000).
12. M. M. Kras'ko, V. V. Voitovych, V. B. Niemash, and A. M. Kraitchinskii, Ukr. J. Phys. **49**, 691 (2004).
13. V. B. Neimash, V. V. Voitovich, M. M. Kras'ko, A. M. Kraitchinskii, O. M. Kabaldin, Yu. V. Pavlovskyi, and V. M. Tsmots', Ukr. J. Phys. **50**, 1273 (2005).
14. V. B. Neimash, V. V. Voitovich, A. M. Kraitchinskii, L. I. Spinar, M. M. Kras'ko, V. M. Popov, A. P. Pokanevych, M. I. Gorodis'kyi, Yu. V. Pavlovskyi, V. M. Tsmots, and O. M. Kabaldin, Ukr. J. Phys. **50**, 492 (2005).
15. A. G. Kazanskii, E. I. Terukov, P. A. Forsh, and J. P. Kleider, Semiconductors **44**, 494 (2010).
16. A. G. Kazanskii, O. G. Koshelev, A. Yu. Sazonov, and A. A. Khomich, Semiconductors **42**, 192 (2008).
17. A. A. Sirenko, J. R. Fox, L. A. Akimov, X. X. Xi, S. Ruvimov, and Z. Liliental-Weber, Solid State Commun. **113**, 553 (2000).
18. A. P. Sokolov and A. P. Shebanin, Sov. Phys. Semicond. **24**, 720 (1990).
19. G. D. Cody, T. Tiedje, B. Abeles, B. Brooks, and Y. Goldstein, Phys. Rev. Lett. **47**, 1480 (1981).
20. P. Mishra and K. P. Jain, Phys. Rev. B **64**, 073304 (2001).
21. A. Morimoto, T. Kataoka, and T. Shimizu, Jpn. J. Appl. Phys. **23**, L812 (1984).
22. S. Y. Shiryaev, J. L. Hansen, P. Kringhoj, and A. N. Larsen, Appl. Phys. Lett. **67**, 2287 (1995).
23. H. Richter, Z. P. Wang, and L. Ley, Solid State Commun. **39**, 625 (1981).
24. H. Cambell and P. M. Fauchet, Solid State Commun. **58**, 739 (1986).

Translated by E. Bondareva